

Vickers Micro-Hardness Studies of Mn^{++} And Cu^{++} Doped Calcium Levo-Tartrate Tetrahydrate Single Crystals

S. R. Suthar¹, H. O. Jethva², M. J. Joshi²

¹Physics Department, Municipal Arts and Urban Science College, Mehsana, India

²Crystal Growth Laboratory, Department of Physics, Saurashtra University, Rajkot, India

Corresponding Author: H. O. Jethva²

Abstract: Calcium tartrate crystals are renowned for its ferroelectric nature. To engineer its properties, calcium levo-tartrate tetrahydrate (CLTT) crystals are doped by Mn^{++} and Cu^{++} . Pure and doped CLTT crystals are grown by the gel method. The Vickers micro-indentation hardness tests are carried out at various applied loads to study the mechanical properties of pure and doped CLTT crystals. As the load increases the values of Vickers micro-hardness decreases. The doped crystals are found to be softer than the pure CLTT crystals. The work hardening coefficient and the standard hardness values are found to be less in Mn^{++} doped CLTT crystals than the Cu^{++} doped CLTT crystals. The yield stress and the first order elastic stiffness constant values are calculated from the micro-hardness values for pure and doped crystals. The Hays and Kendall's approach and Proportional Specimen Resistance (PSR) model are applied for pure and doped CLTT crystals. The effect of doping of Mn^{++} and Cu^{++} on the micro-hardness properties of the CLTT crystals is studied and explained.

Keywords: Vickers micro-hardness, Hays and Kendall's law, Proportional Specimen Resistance (PSR) Model.

Date of Submission: 21-02-2018

Date of acceptance: 05-03-2018

I. Introduction

The ferroelectric nature of calcium tartrate was identified by Gon [1]. The single diffusion gel growth method was used to grow pure and Mn^{++} and Cu^{++} doped calcium levo-tartrate tetrahydrate (CLTT) crystals [2,3]. Hardness is quite interesting and challenging property of materials for engineers and materials scientists. Many methods have been applied for measuring hardness of materials, but the most commonly used form of test is the indentation type [4]. The Vickers micro-hardness testing is one of the predominate types of micro-indentation hardness test. It is very precise and adaptable for testing the softest to hardest types of materials, under the varying loads [5-8].

Various crystals of the large varieties have been tested by the Vickers hardness, for example, metallic crystals [9-11], organic crystals [12-14], non-linear optical materials crystals [15-17], ternary alloy single crystals [18], strontium tartrate crystals [19], Mn doped strontium tartrate crystals [20] and ammonium hydrogen tartrate crystals [21]. Recently, the Vickers micro-hardness studies are reported on semi-organic potassium borosuccinate crystals [22].

The structural, dielectric and FTIR as well as EPR spectroscopic studies are already reported on Mn^{++} doped CLTT crystals by the present authors earlier [2]. Also, the dielectric study of Cu^{++} doped CLTT crystals is reported [3]. Both Mn^{++} and Cu^{++} doped CLTT crystals above the Curie temperature remain in para-electric state and found to obey the Curie-Weiss law.

For any device applications the mechanical properties of crystals are important and hence the aim of the present investigation is to study the effect of Mn^{++} and Cu^{++} doping on various mechanical properties of CLTT crystals, for instance, the variation of Vickers micro-hardness with applied load, the yield stress and the first order elastic stiffness constant. Moreover, the Kick's law is studied and further the Hays and Kendall's law and the Proportional Specimen Resistance (PSR) model have been applied.

II. Experimental

The single diffusion gel growth technique is discussed in detail in our previous papers [2,3]. The presence of the actual amount of dopant was known by the inductively coupled plasma (ICP) technique and, further, the powder X-ray Diffraction (XRD) studies confirmed the orthorhombic structure for pure and doped CLTT crystals, which is reported elsewhere [2,3]. The Vickers micro-hardness tests were conducted using Vaiseshika Vickers micro-hardness tester. First, the sample was brought under the line of micrometer eyepiece and the smooth surface was selected for the indentation. At least, five indentations were made at particular load and the indentations were made minimum five times apart the size of maximum indentation mark to avoid any mutual influence. The diagonal lengths of the indentation impressions were measured by using filer eyepiece of

the least capacity of 0.0001428 mm. From the mean diagonal length (d), the Vickers hardness number, H_v , was calculated using the formula
$$H_v = \frac{1.854 P}{d^2} \quad (1)$$

Here, P is the applied load in Newton and d is the mean diagonal length in meter giving the Vickers hardness in MPa, however, the conventional unit is kg/mm^2 . The average value of the Vickers micro-hardness was obtained and the experiment was repeated for other load values. In the present work, 10 s indentation time was kept constant and the loads were selected as 5g, 10g, 15g, 20g, 30g and 50g. The indentation marks produced on {110} crystallographic face were square in shape as shown in Fig. 1(a) and (b) at 5g load and 10g load for pure and 0.103% Mn⁺⁺ doped CLTT crystals, respectively.

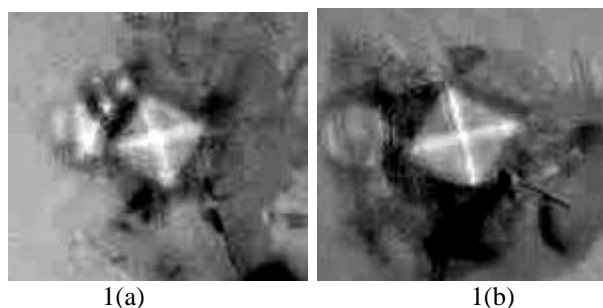


Figure 1: Vickers micro-hardness indentation marks observed for (a) 5g load for pure CLTT and (b) for 10g load for Mn⁺⁺ doped CLTT crystals

III. Result And Discussion

The impurity has prominent effect on hardness. It is a well-known fact that dilute addition of divalent impurity has an appreciable effect on the hardness of alkali halide crystals. For each divalent ion introduced in to the lattice a positive ion vacancy is formed and these defects are distributed in various ways. The impurity ions and vacancies could be present as individual defects independent of one another or they may be present as impurity vacancy complexes or as larger aggregates. All these defects act as obstacles for dislocation motion, therefore, increasing the hardness of the crystals. Rao and Haribabu [23] have studied the effect of the distributed impurities and their state of dispersion on hardness of crystals from micro-hardness measurements on KCl crystals doped with Ca, Ba and Sr. It has been observed that the small addition of impurities increases the hardness; whereas at high concentration of impurity the visible precipitates are observed which result in the decrease of hardness [23]. Altogether, the variation of Vickers micro-hardness with load is studied for potassium dihydrogen phosphate (KDP) crystals grown with organic additives and it is found that the hardness values increase for different additive values [24].

3.1 Effect of load on micro-hardness

The variation of Vickers micro-hardness with load is shown in Fig. 2 and Fig. 3 for Mn⁺⁺ and Cu⁺⁺ doped CLTT crystals, respectively.

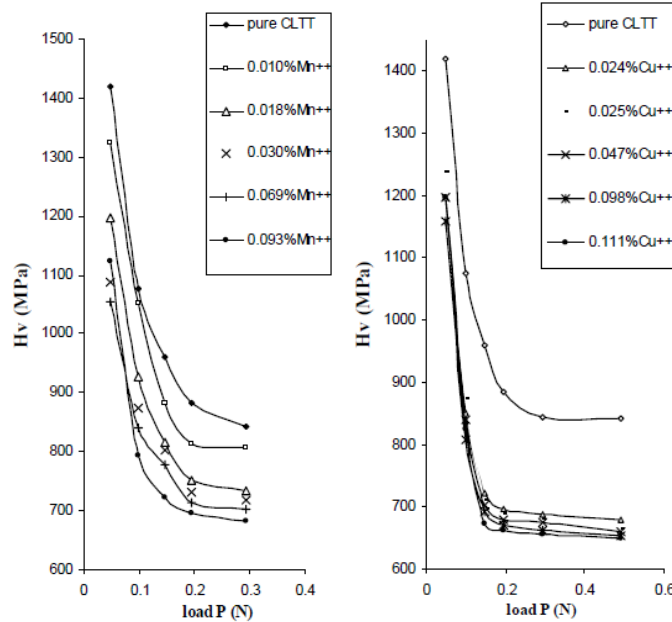


Figure 2

Figure 3

Figure 2: Plots of H_V versus P for pure and Mn^{++} doped CLTT crystals

Figure 3: Plots of H_V versus P for pure and Cu^{++} doped CLTT crystals

From these figures it is observed that as the load increases, initially, the value of hardness decreases rapidly and thereafter, becomes constant. During the indentation, the indenter first penetrates the distorted zone of the surface layer and then the inner layers. Therefore, one observes a decrease in the hardness of the material for increasing the load. As the depth of indentation increases with load, the effect of the inner layers become more and more prominent than the surface layer and as the indenter reaches a depth at which undistorted materials exist and hence no change is observed in the value of hardness with load [25].

From Fig. 2 and Fig. 3, it can be observed that as the amount of doping of Mn^{++} and Cu^{++} increases in CLTT crystals the micro-hardness value decreases at high load regions. The doping of metallic ion impurity facilitates the slip mechanism and makes the sample softer. In the low load regions the resistance offered by the material may be comparable with the applied loads, resulting in a higher value of micro-hardness. However, at higher loads the plastic flow of the material may be higher and hence the resistance offered by the material is small and, therefore, the value of micro-hardness decreases with increase in the value of applied loads and finally becomes constant.

The micro-hardness is related to yield stress (σ_y) by empirical relation $H = 2.38 \sigma_y$ (2)

This has been used for the materials that do not work harden appreciably [26]. The yield stress values are calculated for high load region for pure and Mn^{++} and Cu^{++} doped CLTT crystals and compiled in Table 1.

The yield stress value decreases on increasing the dopant concentration in CLTT crystals. The yield strength indicates the stress at which the crystals start to deform plastically. The reduction in the value of yield stress on doping suggests more plastic deformation in the crystals. The higher value of yield stress for pure CLTT crystal suggests higher resistance to plastic deformation.

Table 1: The values of yield stress (σ_y) and first order elastic stiffness constant (C_{11})

Sample	Yield Stress σ_y (MPa)	First order elastic stiffness constant C_{11} (MPa)
Pure CLTT	280.72	131655.50
0.010% Mn^{++}	266.63	120307.98
0.018% Mn^{++}	241.45	101135.95
0.030% Mn^{++}	233.84	95627.88
0.069% Mn^{++}	228.37	91747.83
0.093% Mn^{++}	228.37	91747.83
0.024% Cu^{++}	226.59	90499.58
0.025% Cu^{++}	221.38	86883.49
0.047% Cu^{++}	219.68	85719.52
0.098% Cu^{++}	218.00	84575.52
0.111% Cu^{++}	216.33	83451.07

The first order elastic stiffness constant (C_{11}) has been evaluated for pure and Mn^{++} and Cu^{++} doped CLTT crystals using Wooster's empirical relation [27];

$$\log C_{11} = \left(\frac{7}{4}\right) \log H_v \tag{3}$$

Where, H_v is the constant micro-hardness.

The values of the first order stiffness constants are given in the Table 1. The values of the first order stiffness constants are comparatively low in the doped crystals than the pure CLTT crystals. The higher value of first order stiffness constant for pure CLTT crystal indicates the stiffer material, which exhibits the smaller elastic strain that results from the application of a given stress. The reduction in the elastic stiffness constant on doping in CLTT crystals indicates more flexibility of the doped crystals. This further suggests that the pure CLTT crystal is stiffer, harder and exhibits less plastic deformation in comparison to the doped crystals.

3.2 Application of Kick's law

The variation of micro-hardness with applied load is explained for the pyramidal Vickers indenter by Kick's law:

$$\log P = \log a + n \log d \text{ or } P = a d^n \tag{4}$$

Where, P is the applied load, a is a constant known as standard hardness, d is the observed diagonal length of indentation and n is a constant for a given material. If $n < 2$, the micro-hardness increases with decreasing the load and if $n > 2$, then the micro-hardness decreases with decreasing the load. Moreover, according to Onitsch [28] and Hanneman [29], the value of n lies between 1.0 and 1.6 for the harder materials and above 1.6 for the softer materials. In order to analyze the indentation size effect (ISE) in the hardness testing, one needs to fit the experimental data as per the Kick's law.

Fig. 4, Fig. 5 and Fig. 6 show the plots of $\log P$ versus $\log d$ for pure CLTT, 0.0103% Mn^{++} doped CLTT and 0.024% Cu^{++} doped CLTT crystals, respectively. Similarly, the plots were drawn for the remaining crystals but not presented here. The values of work hardening coefficient n and constant a are compiled in Table 2. One can observe from the Table 2 that the value of n is slightly higher than 1.6 for pure CLTT and Mn^{++} doped CLTT crystals, however, for Cu^{++} doped CLTT crystals, it is slightly less than 1.6. This indicates that the pure and doped CLTT crystals are at transition point of soft to hard materials. Therefore, further analysis is carried out by using modified relations in the following sections pertaining to the Hays and Kendall's relation and PSR model.

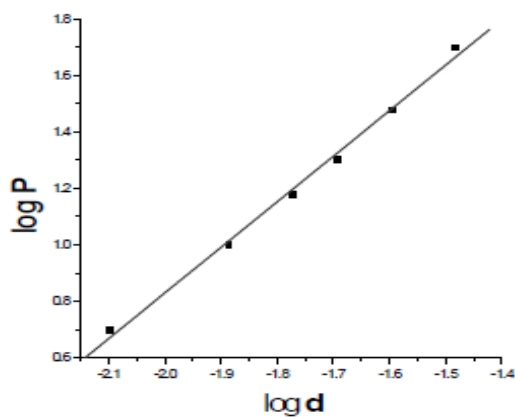


Figure 4: Plot of $\log P$ versus $\log d$ for pure CLTT crystals 0.0103%

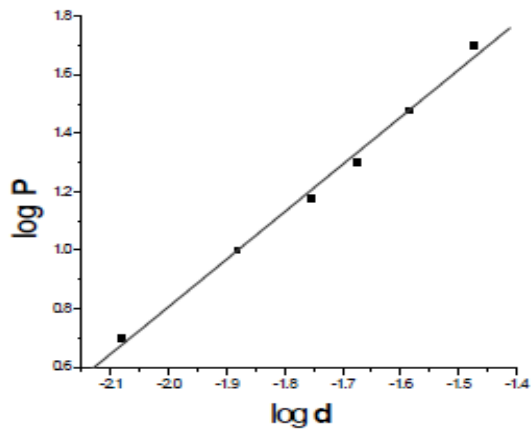


Figure 5: Plot of $\log P$ versus $\log d$ for Mn^{++} doped CLTT crystals

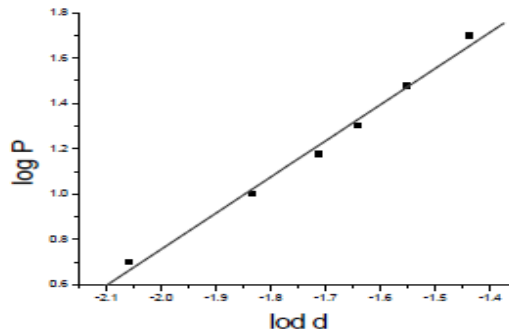


Figure 5: Plot of $\log P$ versus $\log d$ for 0.024% Cu⁺⁺ doped CLTT crystals

Table 2: The values of n and a

Sample	Work hardening coefficient n	Constant a in g
Pure CLTT	1.62	11486.82
0.010% Mn ⁺⁺	1.62	11043.33
0.018% Mn ⁺⁺	1.63	10597.42
0.030% Mn ⁺⁺	1.67	12164.66
0.069% Mn ⁺⁺	1.68	12251.80
0.093% Mn ⁺⁺	1.63	10099.50
0.024% Cu ⁺⁺	1.59	8845.04
0.025% Cu ⁺⁺	1.56	7748.18
0.047% Cu ⁺⁺	1.58	8163.94
0.098% Cu ⁺⁺	1.59	8517.26
0.111% Cu ⁺⁺	1.57	7636.60

3.3 Application of Hays and Kendall law

According to the approach of Hays and Kendall [30], the typical load variation can be due to the sample exerting a Newtonian pressure on the loaded indenter. This resultant pressure depends on the type of the material being tested and represents the minimum applied load for indentation without allowing any plastic deformation.

$$P - W = Kd^2 \quad (5)$$

Where, K is the constant, d is the diagonal length, W is the pressure and P is the load.

The plot of P versus d^2 in such a case has a positive intercept on the P -axis, which represents the value of W . The applied load P is reduced by the term ' W ' and the hardness is calculated from the modified relation

$$H_V = 1.8544 \times \frac{P - W}{d^2} \quad (6)$$

This is the load independent value of hardness. Several reports are available on application of Hays and Kendall law to Vickers micro-hardness studies, e.g., $KMgF_3$ crystals [31], calcium titanate and nickel titanate crystals [32], yttrium ortho-ferrite crystal [33], amino acid doped KDP crystal [17]. Fig. 6 and Fig. 7 show the plots of P versus d^2 for pure and Mn⁺⁺ and Cu⁺⁺ doped CLTT crystals.

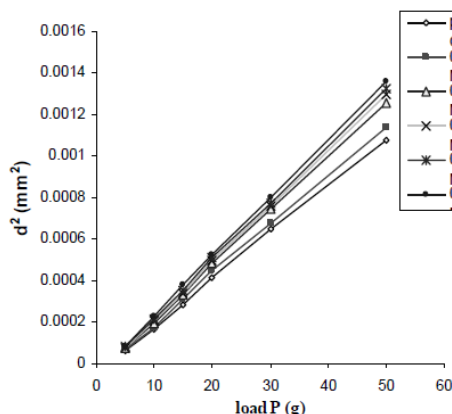


Figure 6

Figure 6: Plot of P versus d^2 for pure and Mn⁺⁺ doped CLTT crystals

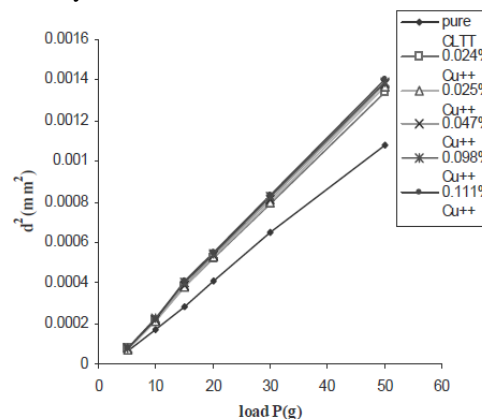


Figure 7

Figure 7: Plot of P versus d^2 for pure and Cu⁺⁺ doped CLTT crystals

In these plots the intercept on load (*P*) axis represents the value of *W*, which is listed in Table 3. The load independent hardness is calculated by using equation (6), which is also compiled in Table 3.

It can be noticed that on increasing the dopant concentration the load independent hardness decreases for both Mn⁺⁺ and Cu⁺⁺ doping in CLTT crystals, which further suggest that the doped CLTT crystals are softer than pure CLTT crystals.

Table 3: Values of load independent *H_V* and Hays and Kendall intercept *W*

Sample	Load independent <i>H_V</i> average in Pa/m ²	Intercept on P axis = <i>W</i> in g
Pure CLTT	800.46	2.24
0.010% Mn ⁺⁺	767.57	2.10
0.018% Mn ⁺⁺	691.64	2.16
0.030% Mn ⁺⁺	668.16	2.09
0.069% Mn ⁺⁺	654.84	2.02
0.093% Mn ⁺⁺	651.40	1.84
0.024% Cu ⁺⁺	662.75	1.93
0.025% Cu ⁺⁺	643.04	2.20
0.047% Cu ⁺⁺	641.41	2.05
0.098% Cu ⁺⁺	639.21	1.39
0.111% Cu ⁺⁺	637.59	1.92

3.4 Proportional Specimen Resistance (PSR) model

The results of a micro-hardness can be influenced by many factors and one of them is the indentation size effect (ISE), in which the observation of phenomenon that the hardness depends on the applied load is considered [34]. Several authors have reported ISE in the Vickers micro-hardness [35-37,17]. The ISE can be explained by the Proportional Specimen Resistance (PSR) model.

According to PSR model, the micro-hardness can be described with two terms, the first term represents the frictional forces between the test specimen and the indenter facets and the second term is concerned with the elastic resistance of the test specimen. The indentation test load *P* is related to indentation size *d* as [38]

$$P = a_1d + a_2d^2 \tag{7}$$

Here, *a₁* coefficient is the contribution of proportional specimen resistance to the apparent micro-hardness and *a₂* coefficient is related to the load independent micro-hardness or load independent constant. The parameter *a₁* characterizes the load dependence of hardness. Li and Bradt [38] suggested that *a₁/a₂* can be considered as a measure of the residual stress and this is connected with defect. The term *a₁d* has been attributed to the energy used in creating new surface such as indenting facets and micro-cracking by Frohlich et al [39] and on the other hand, Li and Bradt [38] related this term to frictional and elastic contribution to PSR model. The term *a₂d²* is considered to be the work for permanent deformation by Frohlich et al [39] or the volume energy of deformation by Li and Bradt [38]. From equation (7), one can write as follows:

$$\frac{P}{d} = a_1 + \left(\frac{P_c}{d_o^2} \right) d \tag{8}$$

Where, *P_C* is the critical applied test load above which micro-hardness becomes load independent and *d_o* is the corresponding diagonal length of the indentation mark. The applicability of the PSR model to describe the observed indentation size effect (ISE) is in relatively wide range of applied test loads, which can be examined by the linearity between *P/d* and *d*. The term *a₂* is not related to the ISE, rather, it is related to the load independent micro-hardness, which is equal to *P_C/(d_o)²*. It should be noted that in the case of *a₁>0*, the normal ISE is obtained where the *H_V* decreases with increase in the load. Notwithstanding, for *a₁<0* a reverse ISE is found, where the *H_V* increases with increase in the load. Applying the PSR model to pure, Mn⁺⁺ and Cu⁺⁺ doped CLTT crystals; it has been observed that the plots of *P/d* versus *d* give straight lines for Mn⁺⁺ 0.0103% doped CLTT crystals as shown in the Fig. 8 and for 0.024% Cu⁺⁺ doped CLTT crystals as shown in the Fig. 9. Similarly, the plots for other samples were drawn but not shown here.

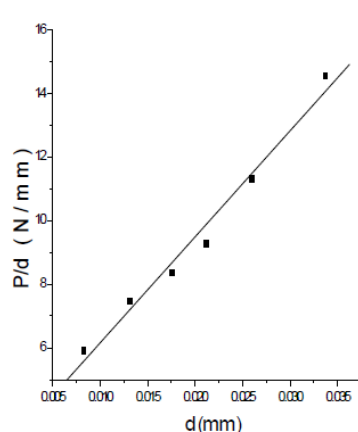


Figure 8

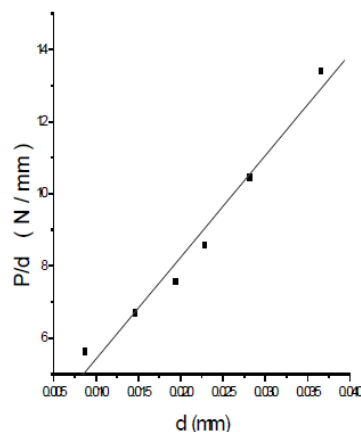


Figure 9

Figure 8: Plot of P/d versus d for 0.0103% Mn^{++} doped CLTT crystals

Figure 9: Plot of P/d versus d for 0.024% Cu^{++} doped CLTT crystals

The linear relation of the plots confirms the applicability of the PSR model to the samples. The values of slope and intercept are obtained from equation (8) and listed in Table 4 for pure, Mn^{++} and Cu^{++} doped CLTT crystals.

Table 4: values of standard hardness and intercept from PSR model for pure, Mn^{++} and Cu^{++} doped CLTT crystals

Sample	Standard hardness $P_C/(d_0)^2$ in MPa	Intercept a in N/mm
Pure CLTT	350.17	2.96
0.010% Mn^{++}	333.32	2.82
0.018% Mn^{++}	304.79	2.65
0.030% Mn^{++}	305.67	2.36
0.069% Mn^{++}	301.23	2.25
0.093% Mn^{++}	288.26	2.31
0.024% Cu^{++}	282.28	2.59
0.025% Cu^{++}	267.50	2.87
0.047% Cu^{++}	270.34	2.69
0.098% Cu^{++}	271.83	2.53
0.111% Cu^{++}	263.35	2.67

From this table, one can observe by and large that as the dopant concentration increases the value of load independent hardness decreases for both Mn^{++} and Cu^{++} doping in CLTT crystals, this again indicates that the crystals become soft on doping.

It has been found that the doping of Mn^{++} and Cu^{++} in CLTT crystals make them softer, however, the Cu^{++} doped CLTT crystals are softer than Mn^{++} doped CLTT crystals. Also, it has been found that the crystals become progressively softer on increasing the doping concentration. It is quite known that the hardness is considered as a measure of the resistance to permanent deformation. This resistance is related to the difficulty of shearing one part of the material over another part. Microscopically, to shear one atom relative to another one requires the re-arrangement of the chemical bonds across the shear plane. If bonds are not localized as it happens in the ionic crystals, the shearing distorts them and offer resistance to the shear. This has been discussed in detail elsewhere [40,17]. It has been found that in the case of transition metal doping the dopants occupy interstitial sites in calcium tartrate tetra hydrate crystals. The three types of structural differences have been observed, which are the shortening of the shortest Ca – O bond constant, difference in torsion angles in tartrate ions and finally hydrogen bond affected by the doping atom localization [41]. The modification in bonding introduced in such a manner by transition metal ion doping, viz. Cu^{++} and Mn^{++} , in CLTT crystals that it is responsible for comparative easy shear and hence the reduction in the Vickers micro-hardness of doped crystals in comparison to pure crystals. This reduction in the shear may differ with transition metal ionic radii, i.e. Mn^{++} (0.8 Å) and Cu^{++} (0.73 Å). The slip in the crystals is expected to be facilitated by comparatively smaller radius cation doping in CLTT crystals. The application of Hays and Kendall relation and PSR model indicate normal ISE in pure and doped crystals.

IV. Conclusion

Due to the doping of Mn^{++} and Cu^{++} in CLTT crystals the Vickers micro-hardness decreases in comparison to the pure CLTT crystals. As the concentration of Mn^{++} and Cu^{++} increases the value of micro-hardness decreases. The Vickers micro-hardness decreases as the applied load increases in the low load range and, thereafter, it becomes virtually independent of load at higher loads. The values of yield stress and first order stiffness constants are lower in Mn^{++} and Cu^{++} doped CLTT crystals than the pure CLTT crystals. This suggests

higher plastic deformation and lesser stiffness of the doped crystals compared to the pure crystals. Applying Kick's law it is found that the values of n are nearby 1.6 indicating the boundary regime of softer to harder material nature. Indentation Size Effect (ISE) has been observed for pure and doped CLTT crystals. By applying Hays and Kendall law and PSR model it has been possible to confirm the normal ISE and reduction in the micro-hardness of CLTT crystals on doping Mn⁺⁺ and Cu⁺⁺. The results of various analysis suggests that the pure CLTT crystal is stiffer, harder and exhibits less plastic deformation in comparison to doped crystals. The doping of Mn⁺⁺ and Cu⁺⁺ in CLTT is expected to modify Ca – O bonds, torsional angle of tartrate ions and hydrogen bonding, which leads to lesser shear resistance and ultimately offers lesser values of hardness in doped crystals compared to the pure crystals.

Acknowledgement

The authors are thankful to Prof. H. H. Joshi, Head, Physics Department, for his keen interest and UGC for SAP DRS-II and DST for FIST. The author (SRS) is thankful to the management of MAUS college, Mehsana, for encouragement.

References

- [1]. H. B. Gon, *J. Cryst. Growth.*, 102, 1990, 501.
- [2]. S. R. Suthar and M. J. Joshi, *Cryst. Res. Technol.*, 41, 2006, 664.
- [3]. S. R. Suthar, S. J. Joshi, B. B. Parekh and M. J. Joshi, *Indian J. Pure and Appl. Phys.*, 45, 2007, 52.
- [4]. A. F. Mohrnhelm, *Micro hardness testing and Hardness numbers in Interpretive Techniques for Micro-structural Analysis* (Springer 1977).
- [5]. H. E. Boyer, *Hardness testing* (ASM Publication 1987).
- [6]. H. Chandler, *Hardness testing* (ASM Publication 1999).
- [7]. J. Edwards, *Hardness testing characterization of materials* (Wiley 2012).
- [8]. J. H. Westbrook and H. Conrad, *The Science of Hardness Testing and its Research Application* (American Society for Metals 1973).
- [9]. M. J. Joshi, *Indian J. Phys.*, 67A, 1993, 353.
- [10]. A. H. Raval, M. J. Joshi and B. S. Shah, *Indian J. Eng. Mater. Sci.*, 9, 2002, 79.
- [11]. D. J. Vaidya, Ph D Thesis, Veer Narmad South Gujarat University, Surat, Gujarat, 2005.
- [12]. M. J. Joshi and B. S. Shah, *Cryst. Res. Technol.*, 19, 1984, 1107.
- [13]. K. Gayathri, P. Krishnan, P. R. Rajkumar and G. Anbalagan, *Bull. Mater. Sci.*, 37, 2014, 1589.
- [14]. J. F. Moxnes, O. Froyland, T. Olsen, T. L. Jensen and E. Unneberg, *Contemp. Eng. Sci.*, 9, 2016, 377.
- [15]. R. Hanumantharao and S. Kalainathan, *Bull. Mater. Sci.*, 36, 2013, 471.
- [16]. D. J. Dave, K. D. Parikh and M. J. Joshi, *Adv. Mater. Res.*, 665, 2013, 174.
- [17]. K. D. Parikh, D. J. Dave, B. B. Parekh and M. J. Joshi, *J. Adv. Phys.*, 5, 2016, 1.
- [18]. D. Shah, G. R. Pandya, S. M. Vyas and M. P. Jani, *Turk. J. Phys.*, 31, 2007, 231.
- [19]. A. R. Patel and S. K. Arora, *J. Mater. Sci.*, 12, 1997, 2124.
- [20]. T. Vijaykumari, C. M. Padma and C. K. Mahadevan, *Int. J. Eng. Res. & Appl.*, 2, 2014, 47.
- [21]. C. C. Desai, *Cryst. Res. Technol.*, 22, 1987, 585.
- [22]. M. Lakshmi Priya, D. Ranjanbabu and R. Ezhil Vizhi, *Mater. Sci. & Eng.*, 73, 2015, 012091.
- [23]. M. L. Rao and V. Haribabu, *Indian J. Pure & Appl. Phys.*, 16, 1978, 821.
- [24]. N. P. Rajesh, V. Kannan, P. Santhana Ranghavan, P. Ramsamy and C. W. Lan, *Mater. Lett.*, 52, 2002, 326.
- [25]. X. Shajan and C. Mahadevan, *Bull. Mater. Sci.*, 27, 2004, 327.
- [26]. M. Neuberger, *Handbook of Electronic Materials Vol. 5* (IFT/Plenum 1971).
- [27]. W. A. Wooster, *Rep. Prog. Phys.*, 1C, 1953, 62.
- [28]. E. M. Onitsch, *Mikroskopie*, 2, 1947, 131.
- [29]. M. Hanneman, *Metall. Manch.*, 23, 1941, 135.
- [30]. C. Hays and E. G. Kendall, *Metallography*, 6, 1973, 275.
- [31]. B. Lal and K. K. Kotru, *Mater. Chem. Phys.*, 78, 2002, 202.
- [32]. V. Gupta, K. K. Bamzai, P. N. Kotru and B. M. Wanklyn, *Mater. Chem. Phys.*, 89, 2005, 64.
- [33]. K. K. Bamzai, P. N. Kotru and B. M. Wanklyn, *IEEE Trans. on magnetic*, 28, 1992, 2353.
- [34]. N. A. Fleck and J. W. Hutchinson, *J. Mech. Phys. Solids*, 49, 2001, 2245.
- [35]. K. Sangwal and B. Surowska, *Mater. Res. Innov.*, 7, 2003, 91.
- [36]. I. N. Budiarsa, *Appl. Mech. Mater.*, 39, 2013, 23.
- [37]. J. Danvu, *J. Adv. Ceramics*, 1(1), 2012, 38.
- [38]. H. Li and R. C. Bradt, *J. Mater. Sci.*, 28, 1993, 917.
- [39]. F. Frohlich, P. Grau and W. Grellmann, *Phys. State Sol.*, (A)42, 1977, 79.
- [40]. J. J. Gilman, *Chemistry and Physics of Mechanical Hardness* (John-Wiley 2009).
- [41]. M. E. Torres, T. Lopez, J. Stockel, X. Solans, M. Garcia-Valles, E. Rodriguez-Castellon and C. Gonzalez-Silingo, *J. Solid. Stat. Chem.*, 163, 2002, 491.

IOSR Journal of Applied Physics (IOSR-JAP) (IOSR-JAP) is UGC approved Journal with SI. No. 5010, Journal no. 49054.

S. R. Suthar" Vickers Micro-Hardness Studies of Mn⁺⁺ And Cu⁺⁺ Doped Calcium Levo-Tartrate Tetrahydrate Single Crystals." IOSR Journal of Applied Physics (IOSR-JAP), vol. 10, no.2, 2018, pp. 05-12.